Vaccine xxx (xxxx) xxx

Contents lists available at ScienceDirect

Vaccine

journal homepage: www.elsevier.com/locate/vaccine

A measles virus-based vaccine induces robust chikungunya virus-specific CD4$^+$ T-cell responses in a phase II clinical trial

Katharina S. Schmitz [a], Anouskha D. Comvalius [a], Nella J. Nieuwkoop [a], Daryl Geers [a], Daniela Weiskopf [b], Katrin Ramsauer [c], Alessandro Sette [b,d], Roland Tschismarov [c], Rory D. de Vries [a], Rik L. de Swart [a,*]

[a] Department of Viroscience, Erasmus MC, Rotterdam, The Netherlands
[b] Center for Infectious Disease, La Jolla Institute for Immunology, La Jolla, CA 92037, USA
[c] Themis Bioscience GmbH, Vienna, Austria, a Subsidiary of Merck & Co., Inc., Rahway, NJ, USA
[d] Department of Medicine, Division of Infectious Diseases and Global Public Health, University of California, San Diego (UCSD), La Jolla, CA 92037, USA

ARTICLE INFO

Keywords:
T-cells
Chikungunya
Measles
Virus
Vector-based vaccines
Vaccination

ABSTRACT

Chikungunya virus (CHIKV) is an alphavirus transmitted by mosquitos that causes a debilitating disease characterized by fever and long-lasting polyarthralgia. To date, no vaccine has been licensed, but multiple vaccine candidates are under evaluation in clinical trials. One of these vaccines is based on a measles virus vector encoding for the CHIKV structural genes C, E3, E2, 6K, and E1 (MV-CHIK), which proved safe in phase I and II clinical trials and elicited CHIKV-specific antibody responses in adult measles seropositive vaccine recipients. Here, we predicted T-cell epitopes in the CHIKV structural genes and investigated whether MV-CHIK vaccination induced CHIKV-specific CD4$^+$ and/or CD8$^+$ T-cell responses. Immune-dominant regions containing multiple epitopes *in silico* predicted to bind to HLA class II molecules were found for four of the five structural proteins, while no such regions were predicted for HLA class I. Experimentally, CHIKV-specific CD4$^+$ T-cells were detected in six out of twelve participants after a single MV-CHIK vaccination and more robust responses were found 4 weeks after two vaccinations (ten out of twelve participants). T-cells were mainly directed against the three large structural proteins C, E2 and E1. Next, we sorted and expanded CHIKV-specific T cell clones (TCC) and identified human CHIKV T-cell epitopes by deconvolution. Interestingly, eight out of nine CD4$^+$ TCC recognized an epitope in accordance with the *in silico* prediction. CHIKV-specific CD8$^+$ T-cells induced by MV-CHIK vaccination were inconsistently detected. Our data show that the MV-CHIK vector vaccine induced a functional transgene-specific CD4$^+$ T cell response which, together with the evidence of neutralizing antibodies as correlate of protection for CHIKV, makes MV-CHIK a promising vaccine candidate in the prevention of chikungunya.

1. Introduction

Chikungunya virus (CHIKV) is an arthropod-borne virus with a single stranded RNA genome of positive polarity, and is a member of the genus *Alphavirus* in the family *Togaviridae*. Humans are the major reservoir species, although the virus can also infect non-human primates. The virus is transmitted by *Aedes albopictus* and *Aedes aegypti* mosquitos, and its life cycle includes replication in both the arthropod and the mammalian host. CHIKV dissemination is therefore limited to the natural habitat of the *Aedes* mosquitos and was originally restricted to Africa and Asia. However, in recent years climate change has extended the habitat of the *Aedes* species to the Americas and Europe, leading to CHIKV cases in these regions [1,2]. CHIKV causes chikungunya fever (CHIKF), an acute febrile illness often accompanied by polyarthralgia that can persist for months to years, frequently causing an inability to work [3]. Chikungunya has a case-fatality rate of <1 %, but the long-term debilitating morbidity causes a large economic burden on public health [4]. Control measures are restricted to the reduction of mosquito populations and prevention of mosquito bites achieved by education of the public, which can be effective if sufficient CHIKV cases are identified [5]. Yet, infections continue to occur in the form of small epidemics in immunologically naive individuals in affected regions.

CHIKV antigenic diversity is limited and only one serotype is recognized. Moreover, virus neutralizing antibodies are generally

* Corresponding author.
E-mail address: r.deswart@erasmusmc.nl (R.L. de Swart).

https://doi.org/10.1016/j.vaccine.2023.09.022
Received 7 April 2023; Received in revised form 5 September 2023; Accepted 12 September 2023

accepted as the correlate of protection from disease, making CHIKV a promising candidate to tackle by vaccination [6–8]. Multiple vaccine candidates have reached different stages of clinical development, with a vaccine based on a measles virus (MV) backbone (MV-CHIK) being one of the most advanced candidates (reviewed in [9]). Measles vaccines were introduced in the 1960s and have averted >23.2 million deaths between 2000 and 2018 [10]. They are safe, and efficacy is as high as 93 % after a single immunization [11]. Measles vaccination induces humoral as well as $CD4^+$ and $CD8^+$ T-cell responses, and protection is considered life-long with limited secondary vaccine failure, making it an ideal vaccine platform [12]. Recombinant MV-based vector vaccines have been generated for multiple pathogens (reviewed in [13]) including Lassa virus, Zika virus as well as SARS-CoV-2. Pre-clinical experiments have confirmed the induction of humoral and cellular responses to not only the vector, but also the transgene [14–17].

MV-CHIK is a recombinant live-attenuated vaccine based on the MV/Schwarz strain, which encodes the structural proteins of CHIKV (C, E3, E2, 6K, and E1) as an additional transcription unit [15]. This vaccine was immunogenic in mice and non-human primates. Additionally, MV-CHIK protected mice from lethal challenge with CHIKV, and induced protection from clinical manifestations of CHIKV infection in non-human primates [15,18]. Phase I and II clinical trials showed that the vaccine is well tolerated and highly immunogenic in humans, with up to 100 % seroconversion rates after two immunizations [19,20]. Moreover, MV-CHIK vaccination also induced antibodies mediating Fc-effector functions [21]. Importantly, antibody induction was independent of pre-existing MV-specific immunity. Whether MV-CHIK induces cellular immune responses to the transgene in humans remains to be investigated.

Here, we detected CHIKV-specific $CD4^+$ and $CD8^+$ T-cells that were induced by MV-CHIK vaccination in human peripheral blood mononuclear cells (PBMC) collected during a phase II clinical trial. These trials were performed in measles-immune adult participants from countries where CHIKV is not endemic. The $CD4^+$ T-cell response was further characterized, and T cell clones (TCC) induced by MV-CHIK vaccination were sorted, expanded, and characterized. HLA-class II-restricted epitopes were experimentally identified and overlapped with *in silico* predicted immune-dominant regions. We conclude that CHIKV-specific $CD4^+$ T-cells are efficiently induced by MV-CHIK and are directed to epitopes in the three major structural proteins C, E2 and E1. In contrast, MV-CHIK-specific $CD8^+$ cytotoxic T-cells could only be identified in a minority of study participants.

2. Material and methods

2.1. Ethics statement

PBMC from healthy adult volunteers enrolled in the phase II clinical study MV-CHIK-205 (ClinicalTrials.gov NCT03635086; EUDRACT no. 2018-000211-25) were collected at various time points as per study protocol. Informed consent allowed for the use of samples for research purposes.

2.2. T-cell epitope prediction

Epitope predictions were performed using TepiTool of the Immune Epitope Database (IEDB; https://tools.iedb.org/tepitool/) as previously described [22]. Briefly, the structural proteins (C, E3, E2, 6K, E1) of the CHIKV sequence of strain 06-49 (GenBank: AM258994.1), encoded by the vaccine, were used for *in silico* predictions. For HLA class II ($CD4^+$ T-cell) binding predictions, we used a prediction rank cut-off <20 and predicted 15-mer epitopes for the 26 most frequent alleles using the IEDB recommended prediction method. HLA class I ($CD8^+$ T-cell) binding predictions were performed using the IEDB recommended class I prediction algorithm for 9-mer epitopes with a prediction cut-off <1 for the 27 most frequent alleles. For the final list displayed in Supplementary Table 1, epitopes were clustered and then filtered to eliminate redundancies and nested peptides.

2.3. Trial design

Participants of the phase II trial MV-CHIK-205 received MV-CHIK, a vaccine candidate for the prevention of chikungunya fever, at a dose of 1×10^6 $TCID_{50}$ per intra-muscular administration on day 0 and 28. Blood samples were collected at 0, 14, 28, 42 and 56 days post vaccination.

2.4. Cells and viruses

Vero cells were cultured in DMEM medium (Lonza, Belgium) supplemented with 1,000 U/ml penicillin, 100 µg/ml streptomycin (Lonza, Belgium), 2 mM L-glutamine (Lonza, Belgium) and 10 % fetal bovine serum (FBS). Donor-specific Epstein Barr Virus (EBV)-transformed lymphoblastic B-cell lines (B-LCL) were generated by infection of donor peripheral mononuclear blood cells (PBMC) collected pre-MV-CHIK-vaccination with EBV. EBV-transformed PBMC were cultured in 96-well roundbottom plates and PHA-L (1 µg/ml) was added initially. Cells were monitored from 14 days onwards and split when they exceeded a density of 3×10^5 cells/well. B-LCL were expanded and maintained in RPMI-1640 medium (Lonza, Belgium) supplemented with penicillin, streptomycin, L-glutamine and 10 % fetal bovine serum (FBS). Donor PBMC were thawed in IMDM (Lonza, Belgium) supplemented with 10% FBS, penicillin, streptomycin, and L-glutamine. PBMC were treated with 50 U/ml Benzonase (Merck) for 30 min at 37 °C prior to use in activation induced marker assay (AIM). CHIKV-specific TCC were maintained in RPMI-1640 medium containing 10% pooled human serum (Sanquin, Rotterdam, the Netherlands), penicillin, streptomycin and L-glutamine (R10H), supplemented with 50 U/ml IL-2. MV-CHIK and the parental MV/Schwarz strain were grown on Vero cells. To this end, Vero cells were inoculated at a MOI of 0.01 and harvested at full CPE. Stock titers were determined by end-point titration and 50% tissue culture infectious dose ($TCID_{50}$) was assessed by the Reed-and-Muench-method.

2.5. Overlapping CHIKV peptide pools

CHIKV peptides were synthesized as crude material (TC Peptide Lab, San Diego, CA). Overlapping 15-mer by 10 amino acids covering the structural proteins of CHIKV C, E3, E2, 6K and E1 were synthesized and individually resuspended in DMSO at a concentration of 10 to 20 mg/ml. Pools for each protein (C, E3, E2, 6K or E1) were generated by pooling aliquots of these individual peptides, undergoing lyophilization, and resuspending in DMSO at 1 mg/ml [23]. The MegaPool, consisting of all protein pools, and the MesoPools, each consisting of 10 individual peptides, were generated by proportional pooling of individual protein pools or individual peptides, respectively.

2.6. Detection of CHIKV-specific $CD4^+$ and $CD8^+$ T cells by AIM assay

AIM was performed as previously described [24]. In short, 1×10^6 PBMC were stimulated with 1 µg/ml MegaPool_CHIKV (MP_CHIKV) in 200 µl R10H in a 96-well roundbottom plate at 37 °C for 20 h. As control, cells were stimulated with an equimolar concentration of DMSO (negative control) or a combination of PMA (50 µg/ml) and ionomycin (500 µg/ml) (positive control). Detection of AIM expressing cells was performed by flow cytometry staining with the following antibodies: anti-CD3, anti-CD4, anti-CD8, anti-CD45RA, anti-CCR7, anti-CD69, anti-CD137, and anti-OX40. LIVE/DEAD Fixable Aqua Dead Cell staining was included in all samples. Samples were acquired on a FACSLyric. Single lymphocytes were gated based on the FSC-A and SSC-A, LIVE $CD3^+$ T-cells were selected, and T-cells were subtyped into $CD3^+CD4^+$ and $CD3^+CD8^+$ cells. Within the $CD4^+$ and $CD8^+$ T-cells, T^{naive} were defined

as CD45RA$^+$CCR7$^+$ and excluded from further analysis. CHIKV-specific T-cells were detected in memory T-cells by co-expression of AIM on CD4$^+$ (OX40$^+$ and CD137$^+$) or CD8$^+$ (CD69$^+$ and CD137$^+$) cells. The DMSO-stimulated sample was used to set the cutoff gate for activation markers, and activation percentages were corrected for the DMSO background. On average, >300,000 cells, and no <60,000 CD3$^+$ T-cells were acquired per sample.

2.7. Generation of CHIKV-specific TCC

To generate CHIKV-specific TCC, PBMC from three donors were stimulated with MP_CHIKV as described above. 20 h post stimulation, live PBMC were stained with LIVE/DEAD Fixable Aqua Dead Cell staining dye, ant-CD3, anti-CD4, anti-CD8, anti-CD69, anti-CD137, and anti-OX40. AIM (double-)positive cells were single cell sorted into round bottom 96-well plates containing a feeder mix and 30 ng/ml OKT3 in R10H. The feeder mix consisted of 33 × 10^6 cells/plate, which were irradiated (X-ray, 40 Gy) PBMC and B-LCL at a 10:1 ratio from at least 2 different donors each. Sorted single TCC were expanded for 14 days. IL-2 was supplemented on day 1 and day 4 after sort, and every 2–3 days thereafter. Half of the medium was replaced on day 4 and day 5 post sort to reduce the level of OKT3 in the cultures. Individual wells were screened microscopically for T-cell outgrowth every 2 days from day 6 onwards. T-cell cultures were split 1:2 when a cell-density of 300,000 cells/well was exceeded. 14 days post sort TCC were evaluated for CHIKV specificity by ELISpot. When specific, T-cell pellets were subjected to a second round of expansion. TCC were once more stimulated with OKT3 in the presence of 22 × 10^6 feeders in T25 flasks, washed at day 4 and frequently supplemented with IL-2. 14 days post second expansion TCC were frozen at 5 × 10^6 cells/vial in 90 % FBS and 10 % DMSO.

2.8. Determination of donor HLA-type

Genomic DNA was extracted from donor B-LCL using a QIAmp DNA Mini Kit (Qiagen) according to the manufacturer's instructions. HLA haplotypes (HLA-DRB, -DQB, -DPB) were commercially (GenDX, Utrecht, the Netherlands) determined for the three donors from which TCC were expanded. *Donor 1:* HLA-DRB1*03:01, HLA-DRB1*04:01, HLA-DRB3*01:01, HLA-DRB4*01:05, HLA-DQB1*02:01, HLA-DQB1*03:01, HLA-DPB1*01:01, HLA-DPB1*04:01; *Donor 2*: HLA-DRB1*01:03, HLA-DRB1*07:01, HLA-DRB4*01:01, HLA-DQB1*02:02, HLA-DQB1*05:01, HLA-DPB1*02:01, HLA-DPB1*04:01; *Donor 3:* HLA-DRB1*07:01, HLA-DRB1*15:01, HLA-DRB4*01:01, HLA-DRB5*01:01, HLA-DQB1*02:02, HLA-DQB1*06:02, HLA-DPB1*04:02, HLA-DPB1*04:01.

2.9. Characterization of CHIKV-specific TCC by ELISpot

A commercially available pre-coated IFNγ-ELISpot (Mabtech) was used to identify CHIKV-specific TCC. 10,000 CD4$^+$ T-cells were co-cultured over night with peptides (MP_CHIKV, Protein Pools, Meso-Pools or individual peptides), equimolar concentrations of DMSO (negative control) or a combination of PMA (50 µg/ml) and ionomycin (500 µg/ml) (positive control) in ELISpot plates. The following day, ELISpot plates were stained according to the manufacturer's instructions and evaluated for reactivity against the specific stimulus. To assess HLA-restrictions or reactivity to MV-CHIK and MV/Schwarz infected cells, B-LCL with only one matching HLA haplotype or autologous B-LCL, respectively, were pulsed with respective peptide overnight or infected for 48 hrs. B-LCL served as antigen presenting cells [25]; infection of B-LCL was verified by flow cytometry using intracellular staining for the MV-nucleoprotein (clone KK2, Millipore). 5,000 antigen presenting cells were co-cultured with 10,000 CD4$^+$ T-cells; as negative control uninfected and unpulsed B-LCL were used. Similarly, CHIKV-specificity of CD8$^+$ T cells was assessed by co-culture with autologous B-LCL pulsed with MP_CHIKV. ELISpot plates were scanned with an ImmunoSpot analyzer.

3. Results

3.1. Prediction of CHIKV T-cell epitopes identifies immune-dominant regions

We predicted vaccine-encoded CHIKV CD4$^+$ and CD8$^+$ T-cell epitopes using TepiTool (IEDB) by ranking CHIKV-specific peptides for best HLA class II and HLA class I binding, respectively (cut-off rank <20 or <1, respectively). Across all five structural CHIKV proteins (i.e. C, E3, E2, 6K and E1), we predicted 3,815 HLA class II and 1,007 HLA class I binding peptides (Fig. 1**a**). Unsurprisingly, in both cases the highest number of binders was detected in the largest protein (E1), while least peptides were predicted in the E3 protein, one of the two small proteins. Interestingly, we predicted more than twice as much HLA class II binding peptides for protein 6K as expected by its size, and comparably less peptides for protein C (Fig. 1**b**). For HLA class I binding peptides, we detected a similar trend, but here the pattern was less pronounced (Fig. 1**c**). Next, we generated CHIKV genome coverage plots for predicted HLA class II and class I binders (Fig. 1**d** and **e**). Immune-dominant regions were identified by an arbitrary cut-off of ≥10 HLA class II binding peptides predicted to start at a minimum of 3 following genome positions. Using this cut-off, we identified 12 HLA class II immune-dominant regions across the genome starting at position 37–43: QAGQLAQ, 303–307: VMRPG, 328–331: KDNF, 365–370: EATDGT, 678–684: HEIILYY, 688–701: YPTMTVVVVSVATF, 760–769: NEQQPLFWLQ, 788–795: PCCCKTLA, 833–842: YSPMVLEMEL, 1121–1124: FGGV, 1155–1165: VEGNSQLQISF, and 1222–1234: ITGGVGLVVAVAA. We were not able to identify such immune-dominant regions for peptides predicted to bind HLA class I, although single epitopes were occasionally predicted more frequently than others across the entire genome (Fig. 1**e**).

3.2. MV-CHIK vaccination mainly induced CD4$^+$ T-cells

To investigate whether MV-CHIK vaccination induced CHIKV-specific T-cells, we examined PBMC from donors after vaccination with MV-CHIK in an AIM flow cytometry assay. We stimulated PBMC from 12 donors that received two administrations of MV-CHIK at a dose of 1 × 10^6 $TCID_{50}$ on day 0 and 28 with a MegaPool of overlapping peptides spanning all vaccine-encoded CHIKV proteins (MP_CHIKV) (Fig. 2**a-j**). Specific activation of CD4$^+$ T cells was measured via cell surface expression of OX40 and CD137 in the CD4$^+$ memory population (compare Fig. 2**g** and **h**) and is shown as background (DMSO) corrected values (Fig. 2**k**). We consistently detected significant induction of CD4$^+$ T-cells across all time points post vaccination. Pre-vaccination (day 0) 1/12 donors had CD4$^+$ T-cells that upregulated OX40 and CD137 after MP_CHIKV stimulation. This increased to 6/12 and 7/12 donors with measurable CHIKV-specific CD4$^+$ T-cells on day 14 and 28 post first vaccination, respectively. The percentage of AIM-positive T-cells decreased between 14 and 28 days post first vaccination, indicative of a contraction phase after primary vaccination. On day 42 (14 days post second vaccination), 8/12 donors had measurable CHIKV-specific T-cells, which further increased to 10/12 donors by day 56 post vaccination (Fig. 2**k**). We additionally calculated the stimulation index (SI) by dividing MP_CHIKV specific responses over the DMSO control (Fig. 2**l**). Only 4 donors had a positive SI 14 days post vaccination, whereas the majority of donors (9/12) was positive by day 56. Importantly, one donor (grey square) which was occasionally low positive by background subtraction did not have a SI ≥2 at any time point, and one donor (grey circle) that had a SI ≥2 at 28 days post vaccination had absolute AIM values below 0.01 %. In this case, this highlights the importance of a combined evaluation of absolute values and SI to define good responders. If a participant was a good responder could not be associated

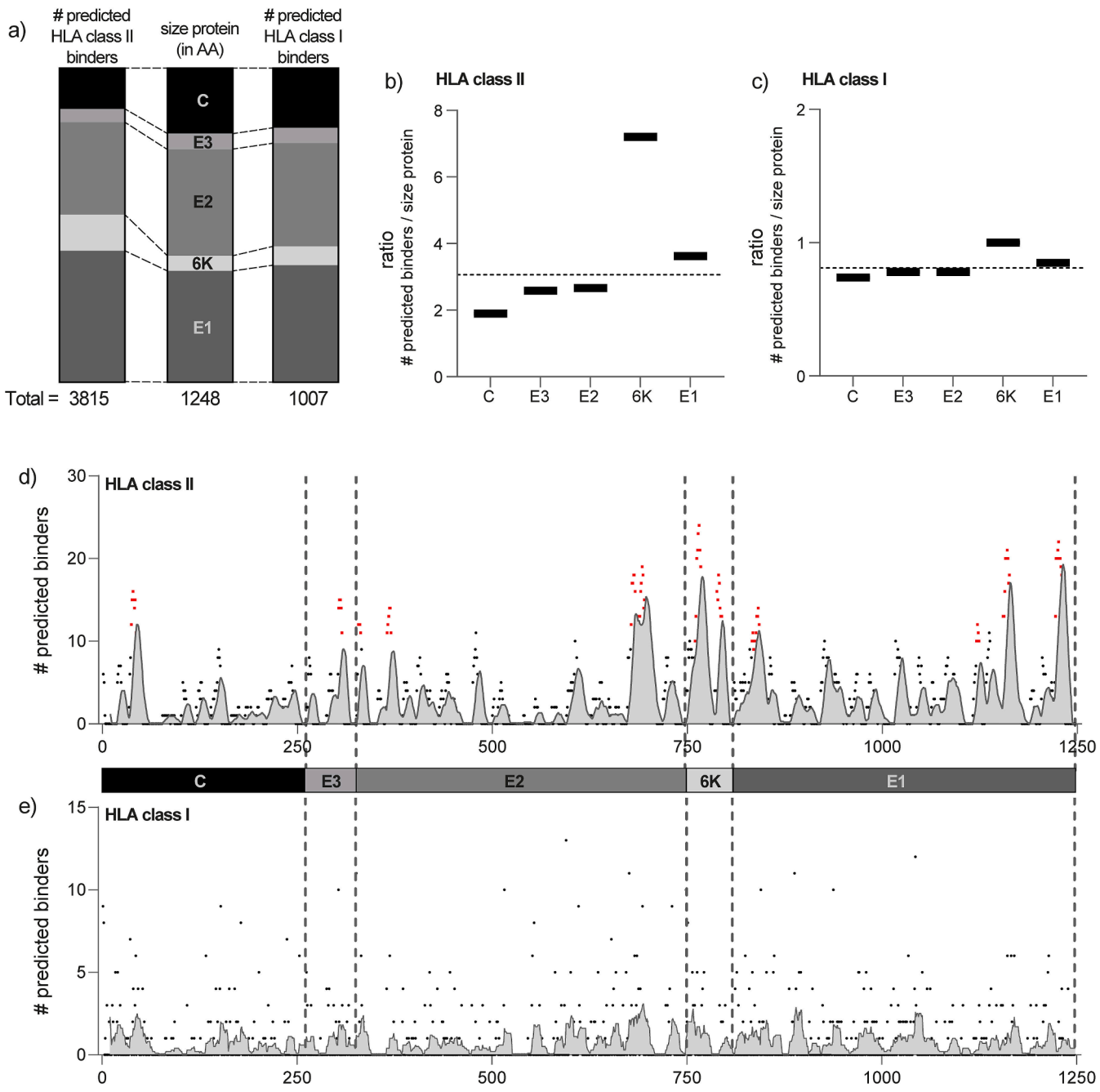

Fig. 1. Predicted CHIKV peptides binding HLA class I and II. a) Relative number of predicted HLA class II (left) and HLA class I (right) binding peptides in comparison to the total size of each structural CHIKV protein. The absolute number of the total predicted peptides/protein size in amino acids (AA) is shown below individual bars. b-c) Ratio between the number of total predicted peptides and the size of each protein for b) HLA class II and c) HLA class I. The dotted line indicates the mean ratio for all predicted peptides across all evaluated proteins. d-e) Coverage plot of predicted d) HLA class II and e) HLA class I binders across the entire genome. Dots indicate the number of predicted peptides starting at each position, grey area shows a sliding average in increments of 10 and red dots highlight start positions of peptides predicted ≥10 times in at least 3 following positions. Vertical dotted lines indicate different proteins.

with other factors.

AIM-positive $CD8^+$ T-cells were defined as $CD69^+CD137^+$ (Fig. 2**m**). In general, a high background of activated $CD8^+$ T-cells after DMSO stimulation was observed, complicating the detection of CHIKV-specific $CD8^+$ T-cells. At most time points, we detected no notable increase in the frequency of AIM-positive $CD8^+$ T cells when comparing peptide stimulated to control samples. The SI was low and only one donor exceeded a SI of 2 at one time point (Fig. 2**n**). Importantly, we did observe an upwards trend over time in background corrected data and SI for three donors (star, grey diamond, half-filled circle), possibly indicating the presence of CHIKV-specific $CD8^+$ T-cells.

3.3. Cloning of CHIKV-specific T-cells led to dominant expansion of $CD4^+$ clones

To identify CHIKV T-cell epitopes, we sorted AIM-positive single $CD4^+$ and/or $CD8^+$ T-cells from 3 and 1 donors, respectively, and expanded TCC. For donor 1 (visit: 42 days post vaccination; star in Fig. 2), we sorted approximately 300 single $CD4^+$ T-cells and 500 single $CD8^+$ T-cells, of which 77 and 47 TCC were successfully expanded, respectively. We tested all TCC in IFNγ-ELISpot for their reactivity to MP_CHIKV. 9 % (7/77) of the $CD4^+$ TCC were specific for CHIKV, while none of the $CD8^+$ TCC appeared to be CHIKV-specific. For donor 2 (visit:

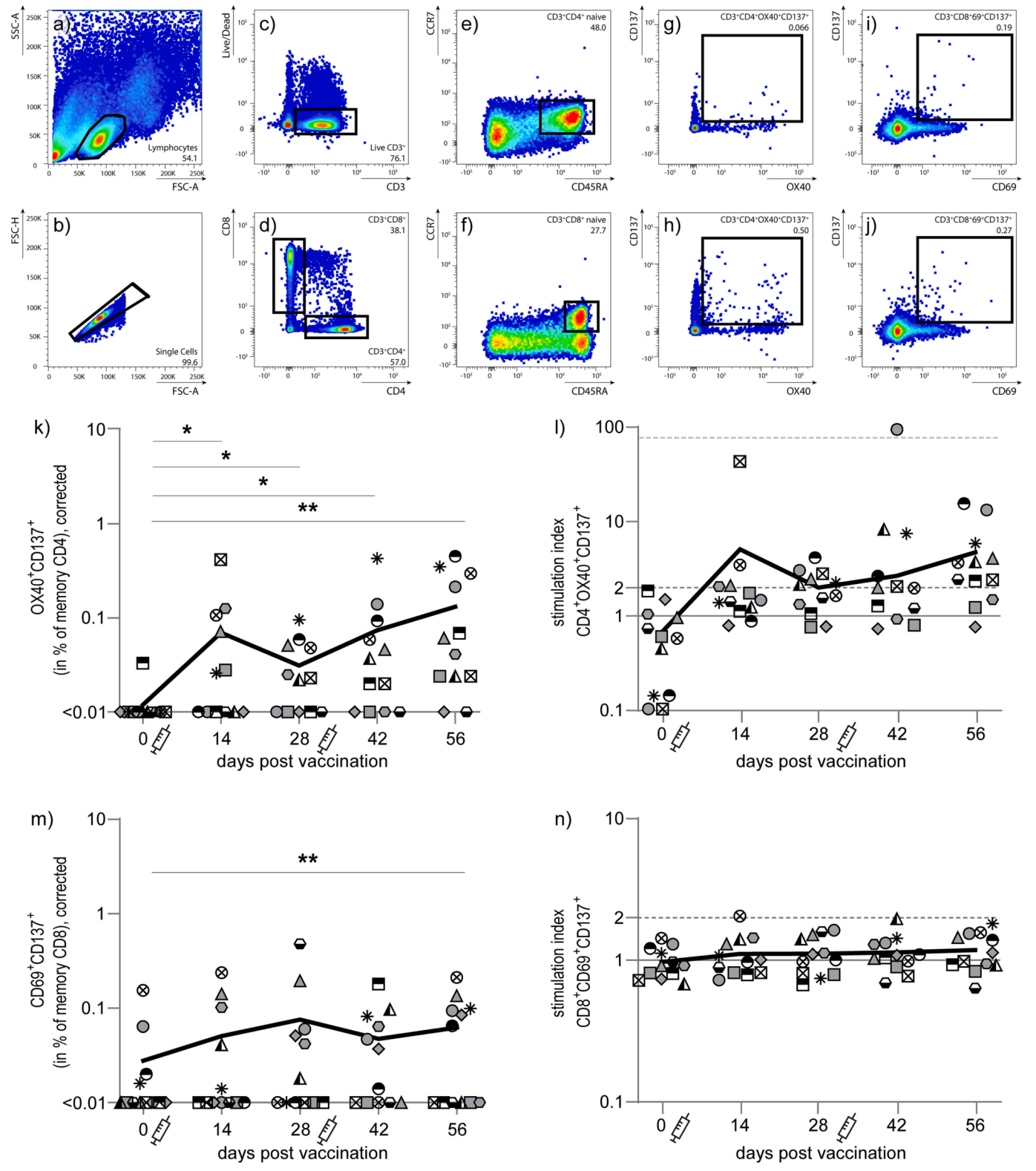

Fig. 2. Detection CHIKV-specific T-cells after MV-CHIK vaccination. a-j) Representative gating strategy: T-cells were defined as lymphocytes (a), single cells (b), live and $CD3^+$-expressing (c). They were further subdivided into $CD4^+$ and $CD8^+$ T-cells (d) and the naive T-cell population, defined as $CCR7^+CD45RA^+$, was excluded for $CD4^+$ (e) and $CD8^+$ (f) T-cells. The remaining memory cells were analysed for their activation induced markers (AIM) CD137 and OX40 in the case of $CD4^+$ (g,h) and CD137 and CD69 in the case of $CD8^+$ (i,j) after DMSO (g, i) or MP_CHIKV (h,j) stimulation. k, m) AIM-positive $CD4^+$ (k) and $CD8^+$ T-cells (m) after background-subtraction for 12 individual donors at 5 different time points pre and post vaccination with MV-CHIK. l, n) Stimulation index (SI) for $CD4^+$ (l) and $CD8^+$ (n) T-cells. The cut-off for positive stimulation was set at a SI of 2. l) The upper dotted line represents an artificial cut-off. The sample above this line is artificially placed there as the AIM value for the DMSO sample was 0 and no SI could be determined. This sample does not contribute to the presented mean. The black lines connecting individual symbols indicate the mean. Individual symbols are consistent throughout the figures. Days of vaccination are indicated as syringe symbol.

56 days post vaccination; grey circle in Fig. 2) and donor 3 (visit: 42 days post vaccination; half-filled triangle in Fig. 2), we exclusively sorted CD4$^+$ T-cells. 14 % of donor 2 TCC and 10 % of donor 3 TCC expanded of which 44 % (11/25) and 1 % (1/9) were CHIKV-specific, respectively.

3.4. CHIKV-specific CD4$^+$ TCC recognize epitopes in CHIKV C, E2 and E1 protein

Next, we determined the minimal 15-mer epitopes for all 19

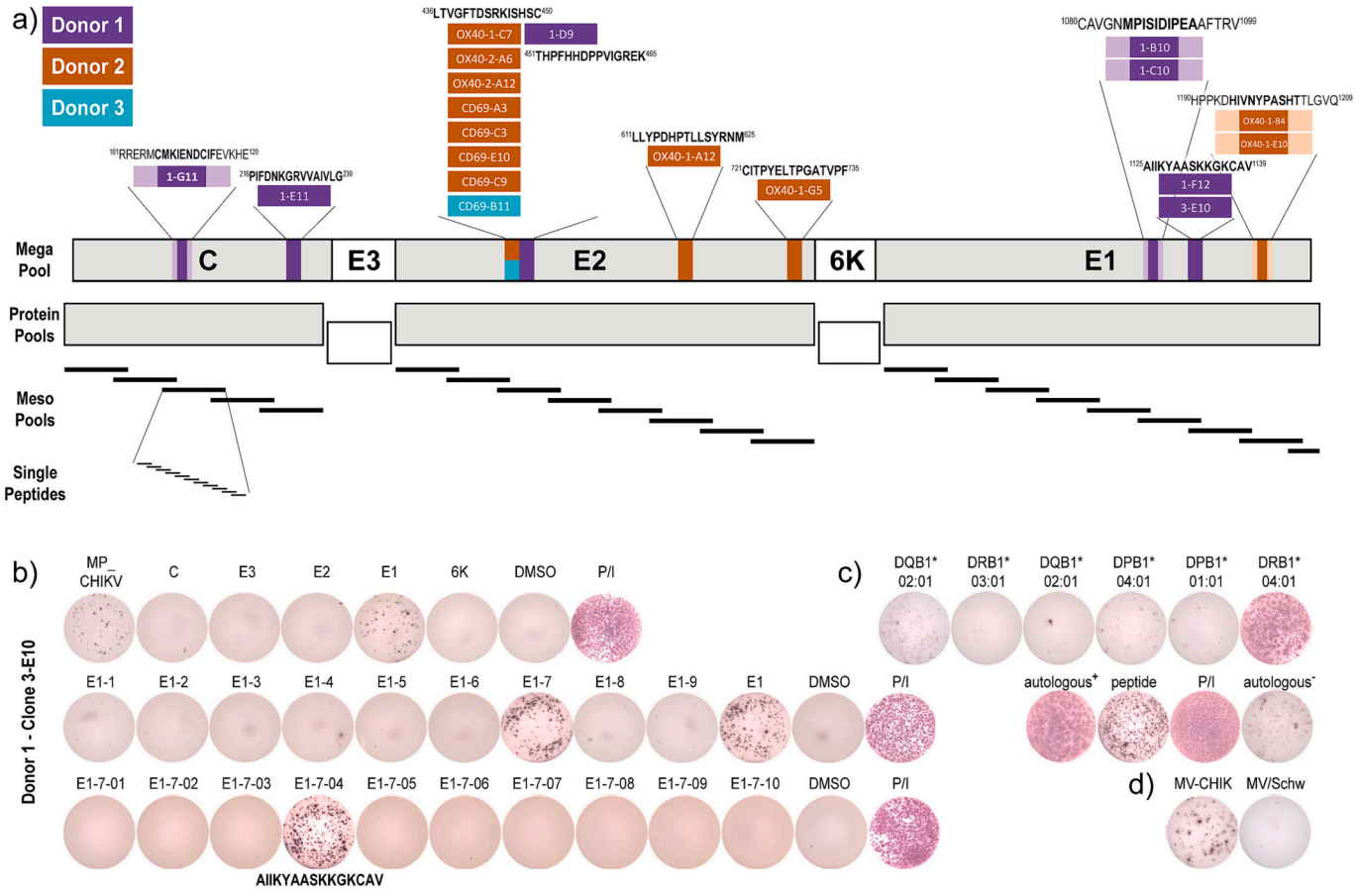

e)

Donor	Clone	Mega Pool	Protein Pool	Meso Pool	Single Peptide	Peptide sequence	HLA-restriction	rxn to MV-CHIK	rxn to MV/Schw
Donor 1	**1 - G11**	x	C	3	32, 33	RRERMCMKIENDCIFEVKHE	HLA-DRB1*03:01	no	no
	1 - E11	x	C	5	55	PIFDNKGRVVAIVLG	HLA-DQB1*03:01	yes	no
	1 - D9	x	E2	3	88	THPFHHDPPVIGREK	HLA-DRB1*04:01, HLA-DRB1*03:01	yes	no
	1 - B10	x	E1	6	211,212	CAVGNMPISIDIPEAAFTRV	HLA-DRB1*03:01, HLA-DQB1*03:01	yes	no
	1 - C10	x	E1	6	211,212	CAVGNMPISIDIPEAAFTRV	HLA-DRB1*03:01	yes	no
	1 - F12	x	E1	7	220	AIIKYAASKKGKCAV	HLA-DRB1*04:01	yes	no
	3 - E10	x	E1	7	220	AIIKYAASKKGKCAV	HLA-DRB1*04:01	yes	no
Donor 2	**OX40 - 1-C7**	x	E2	3	85	LTVGFTDSRKISHSC	HLA-DRB1*07:01, HLA-DQB1*02:02	yes	no
	OX40 - 2-A6	x	E2	3	85	LTVGFTDSRKISHSC			
	OX40 - 2-A12	x	E2	3	85	LTVGFTDSRKISHSC	HLA-DRB1*07:01, HLA-DQB1*02:02	yes	no
	CD69 - A3	x	E2	3	85	LTVGFTDSRKISHSC	HLA-DRB1*07:01, HLA-DQB1*02:02	yes	no
	CD69 - C3	x	E2	3	85	LTVGFTDSRKISHSC			
	CD69 - E10	x	E2	3	85	LTVGFTDSRKISHSC	HLA-DRB1*07:01, HLA-DQB1*02:02	yes	no
	CD69 - C9	x	E2	3	85	LTVGFTDSRKISHSC			
	OX40 - 1-A12	x	E2	6	120	LLYPDHPTLLSYRNM	HLA-DRB1*07:01, HLA-DQB1*02:02	yes	no
	OX40 - 1-G5	x	E2	8	142	CITPYELTPGATVPF	HLA-DRB1*07:01, HLA-DQB1*02:02	yes	no
	OX40 - 1-B4	x	E1	8	233/234	HPPKDHIVNYPASHTTLGVQ	HLA-DRB1*15:01	yes	no
	OX40 - 1-E10	x	E1	8	233/234	HPPKDHIVNYPASHTTLGVQ	HLA-DRB1*15:01	yes	no
Donor 3	**CD69 - B11**	x	E2	3	85	LTVGFTDSRKISHSC			

Fig. 3. CHIKV-specific CD4$^+$ TCC are directed against epitopes in the three large CHIKV structural proteins. a) Schematic representation describing the peptide deconvolution process and showing the reactivity of individual TCC of three different donors. TCC that are shown as dark bar with neighbouring light bars were reactive to two overlapping peptides. The MegaPool was used to sort and identify individual TCC and each clone was then systematically tested with all five different protein pools, the corresponding MesoPools (10 individual peptides) and subsequently the 10 different individual peptides in ELISpot. This process is representatively shown for clone 3-E10 in (b). DMSO and the aspecific stimulus PMA/Ionomycin (P/I) were included as controls. c) For each TCC-peptide combination the HLA-restriction was determined using co-cultures of the respective TCC and antigen presenting B-LCL only matching one of the donors HLA-haplotypes. Co-cultures with autologous B-LCL incubated with peptide, peptide only and P/I were used as positive control, co-cultures with autologous B-LCL without peptides were used to determine the background signal. d) TCC were tested for their reactivity against live virus infected cells. Autologous B-LCL were infected with MV/CHIK or MV/Schwarz and then co-cultured with individual TCC in an ELISpot. e) Summary table describing the reactivity, peptide sequence, HLA-restriction and the reactivity to live virus for each individual TCC.

MP_CHIKV-specific CD4$^+$ TCC (Fig. 3**a, b**). To this end, we deconvoluted all TCC against the 5 protein pools (C, E3, E2, 6K, E1), followed by the corresponding MesoPools (containing 10 overlapping peptides), followed by single 15-mer peptides in IFNγ-ELISpot (example presented for clone 3-E10 in Fig. 3**b**). TCC from donor 1 recognized epitopes in the three large structural CHIKV proteins C, E2 and E1 (Fig. 3**a**). Donor 2 TCC recognized epitopes in the CHIKV E2 and E1 protein. Interestingly, 7/11 isolated TCC from donor 2 were directed against the same epitope, indicating efficient clonal expansion. Moreover, the only CHIKV-specific TCC isolated from donor 3 recognized that same epitope in protein E2 (^{436}LTVGFTDSRKISHSC^{450}), possibly indicating an immune-dominant epitope. Similarly, three other epitopes located in E1 were recognized by more than one TCC from the same donor, further evidence for recent clonal expansion.

Next, to determine the HLA restrictions of the expanded TCC, we determined the HLA genotype for the three donors from which TCC were isolated, and tested the clone-specific 15-mer peptides in co-cultures of TCC and different antigen presenting cells only matching one of the donors' HLA molecules (example presented for clone 3-E10 in Fig. 3**c**). As expected, CHIKV TCC from different donors were restricted to a variety of different HLA haplotypes including DRB1*03:01, DRB1*04:01, DRB1*07:01, DRB1*15:01, DQB1*03:01, DQB1*02:02 (Fig. 3**e**). When searching the allele frequency net database [26] for the frequency of the HLA haplotypes of the three donors, we found on average a >10 % allele frequency for populations living in regions endemic for CHIKV like Latin America, USA, Africa, Southern Europe and South-East Asia (data not shown). While DRB1*03:01 was relatively evenly distributed throughout all regions, there were large differences between countries and regions for DRB1*07:01. Generally, DRB1*04:01 and DQB1*02:02 seemed to be less prevalent and DQB1*03:01 more prevalent than average. The different alleles were underrepresented in Sub-Saharan Africa when compared to the other regions. Importantly, 5/6 HLA haplotypes (DRB1*03:01, DRB1*04:01, DRB1*07:01, DRB1*15:01, DQB1*03:01) shown to be relevant in the presentation of CHIKV-peptides for those three donors were also used for initial epitope predictions (Supplementary Table 1).

We compared the experimentally defined epitopes and their HLA-restrictions to predicted CD4$^+$ T cell epitopes. We did not detect any

Table 1
Comparison experimentally determined and predicted epitopes. HLA types printed in bold match experimentally determined HLA type.

Protein	Experimentally identified epitope	Experimentally identified HLA-type	closest predicted epitope	Best HLA binders (cut-off rank <20)
C	PRERMCMKIENDCIFEVKHE	HLA-DRB1*03:01	ERMCMKIENDCIFEV	**HLA-DRB1*03:01**, HLA-DRB3*01:01, HLA-DQA1*05:01/DQB1*02:01, HLA-DQA1*01:01/DQB1*05:01, HLA-DQA1*04:01/DQB1*04:02
			RMCMKIENDCIFEVK	**HLA-DRB1*03:01**, HLA-DRB3*01:01, HLA-DQA1*01:01/DQB1*05:01, HLA-DQA1*04:01/DQB1*04:02
			MCMKIENDCIFEVKH	**HLA-DRB1*03:01**, HLA-DRB3*01:01, HLA-DQA1*04:01/DQB1*04:02
	PIFDNKGRVVAIVLG	HLA-DQB1*03:01	PIFDNKGRVVAIVLG	HLA-DRB3*02:02, HLA-DRB1*13:02, HLA-DQA1*05:01/**DQB1*03:01**, HLA-DQA1*01:02/DQB1*06:02
E2	THPFHHDPPVIGREK	HLA-DRB1*04:01, HLA-DRB1*03:01	CTHPFHHDPPVIGRE	HLA-DRB3*02:02, **HLA-DRB1*03:01**, **HLA-DRB1*04:01**, HLA-DRB3*01:01
	LTVGFTDSRKISHSC	HLA-DRB1*07:01, HLA-DQB1*02:02	TLTVGFTDSRKISHS	**HLA-DRB1*07:01**, HLA-DRB1*11:01, HLA-DRB1*03:01, HLA-DRB5*01:01
	LLYPDHPTLLSYRNM	HLA-DRB1*07:01, HLA-DQB1*02:02	MLLYPDHPTLLSYRN	HLA-DRB3*02:02, HLA-DRB1*13:02, HLA-DRB1*03:01, HLA-DRB1*04:01, HLA-DRB1*15:01, HLA-DRB3*01:01
	CITPYELTPGATVPF	HLA-DRB1*07:01, HLA-DQB1*02:02	ITPYELTPGATVPFL	HLA-DRB3*02:02, HLA-DRB1*09:01, **HLA-DRB1*07:01**, HLA-DRB1*01:01, HLA-DQA1*05:01/DQB1*03:01
E1	HPPKDHIVNYPASHTTLGVQ	HLA-DRB1*15:01	HPPKDHIVNYPASHT	HLA-DRB3*02:02, **HLA-DRB1*15:01**, HLA-DRB1*08:02
			PPKDHIVNYPASHTT	HLA-DRB3*02:02, **HLA-DRB1*15:01**, HLA-DRB1*08:02
			PKDHIVNYPASHTTL	HLA-DRB3*02:02, HLA-DRB1*09:01, **HLA-DRB1*15:01**, HLA-DRB1*08:02
			KDHIVNYPASHTTLG	HLA-DRB3*02:02, HLA-DRB1*09:01, **HLA-DRB1*15:01**, HLA-DRB1*08:02
	CAVGNMPISIDIPEAAFTRV	HLA-DRB1*03:01, HLA-DQB1*03:01	GNMPISIDIPEAAFT	HLA-DRB1*13:02, **HLA-DRB1*03:01**, HLA-DRB1*04:01, HLA-DRB3*01:01, HLA-DQA1*05:01/DQB1*02:01, HLA-DQA1*03:01/DQB1*03:02, HLA-DQA1*04:01/DQB1*04:02
			NMPISIDIPEAAFTR	HLA-DRB3*02:02, HLA-DRB1*13:02, **HLA-DRB1*03:01**, HLA-DRB1*04:01, HLA-DRB3*01:01, HLA-DQA1*05:01/DQB1*02:01, HLA-DQA1*03:01/DQB1*03:02, HLA-DQA1*04:01/DQB1*04:02
			MPISIDIPEAAFTRV	HLA-DRB3*02:02, HLA-DRB1*13:02, **HLA-DRB1*03:01**, HLA-DRB1*04:01, HLA-DRB3*01:01, HLA-DQA1*05:01/DQB1*02:01, HLA-DQA1*05:01/**DQB1*03:01**, HLA-DQA1*03:01/DQB1*03:02
	AIIKYAASKKGKCAV	HLA-DRB1*04:01,	VAIIKYAASKKGKCA	HLA-DRB3*02:02, HLA-DRB1*09:01, HLA-DRB1*07:01, HLA-DRB1*01:01, HLA-DRB1*11:01, **HLA-DRB1*04:01**, HLA-DRB1*15:01, HLA-DRB5*01:01, HLA-DRB1*08:02, HLA-DRB4*01:01

TCC recognizing an epitope in a region that we considered immune-dominant (Fig. 1) based on the number of predicted epitopes starting at the same position. However, we were able to find identical or very similar epitopes in the list of predicted $CD4^+$ T-cell epitopes as we had experimentally determined (Table 1). Strikingly, all but one peptide (LLYPDHPTLLSYRNM) were predicted to bind a HLA molecule that we had also found experimentally.

3.5. CHIKV-specific $CD4^+$ TCC can recognize live virus infected cells

Finally, we investigated the capacity of the isolated TCC to recognize CHIKV-infected cells in addition to peptide-pulsed cells. We infected autologous B-LCL with MV-CHIK and MV/Schwarz and co-cultured them with different TCC overnight in IFNγ-ELISpot plates (example presented for clone 3-E10 in Fig. 3**d**). With the exception of one clone, all tested TCC recognized MV-CHIK but not MV/Schwarz infected cells (Fig. 3**e**).

4. Discussion

Given its debilitating impact, CHIKV has long been recognized as a pathogen of global concern. Moreover, climate change and the associated larger vector distribution increased the need for safe and effective CHIKV vaccines. MV-CHIK has been successfully used in phase I and II clinical trials, and the induction of CHIKV-specific (neutralizing) antibodies, suggested to be a correlate of protection from disease [7], was previously shown [19–21]. MV-CHIK is a recombinant live attenuated vaccine based on the MV/Schwarz vaccine strain that is known to efficiently induce MV-specific T-cells. Here, we show the induction of functional CHIKV-specific $CD4^+$ T-cells by vaccination with MV-CHIK. We predicted $CD4^+$ T-cell epitopes and experimentally identified T-cells induced by vaccination recognizing all major structural CHIKV proteins.

The role of virus-specific T-cells in CHIKV clearance or pathogenicity is controversial [27,28]. Early after acute infection, a $CD8^+$ T-cell response can be detected, but this shifts to a dominant $CD4^+$ T-cell response at later stages [29,30]. During the chronic phase of disease, infiltrating synovial $CD4^+$ (but rarely $CD8^+$) T-cells are associated with inflammation and joint swelling, and were shown to release proinflammatory cytokines [31,32]. CHIKV-specific T-cells could also be detected in the majority of convalescent patients, displaying a $CD8^+$ over a $CD4^+$ phenotype and targeting E2, nsP1 and C [33]. However, it could not be demonstrated that those T-cells had a protective role. Moreover, a number of different vaccine candidates were previously shown to induce specific $CD4^+$ as well as $CD8^+$ T-cells in mouse models (reviewed in [34]). A few of those studies identified CHIKV $CD4^+$ T-cell epitopes in the structural E1 and/or E2 protein [35,36]. Immune-dominant regions were observed in the first and last third of the E1 protein, of which the latter is in line with our data [37,38]. Similarly, another immune-dominant region was determined to be in the end of the first half as well as in the last tenth of the E2 protein, both locations in which we also isolated TCC. Importantly, none of those studies demonstrated the necessity of T-cells for protection [39]. In non-human primates, CHIKV-specific T-cell data are scarce and contentious. A recombinant CHIKV-vaccine based on Eilat virus (EILV/CHIKV) failed to induce detectable CHIKV-specific T-cells in cynomolgus macaques [40]. An attenuated strain of CHIKV (Δ5nsP3) mainly induced E1 and E2-recognizing T-cells with a $CD4^+$ phenotype [41], while five consecutive CHIKV DNA vaccinations led to the induction of specific $CD8^+$ T-cells in three out of four rhesus macaques [42]. A human trial of CHIKV-ChAdOx1 showed the induction of E1 and E2-specific $CD4^+$ T-cells but failed to detect significant $CD8^+$ T-cell responses [43]. In line, we show the induction of CHIKV-specific $CD4^+$ T-cells after MV-CHIK vaccination, but virus-specific $CD8^+$ T-cell responses were hardly detected. Detection and isolation of CHIKV-specific $CD8^+$ T-cells was additionally aggravated by a high background. We have previously observed a higher baseline activation for $CD8^+$ when compared to $CD4^+$ T-cells, but the low frequency of CHIKV-specific $CD8^+$ T-cells makes sensitive detection challenging. Interestingly, we were also not able to *in silico* predict immune-dominant regions for MHC class I binding epitopes across all five structural CHIKV proteins. This is in contrast to Lopes-Ribeiro *et al.* who previously identified a number of reactive CHIKV-peptides in a peptide microarray in the context of HLA-A*02:01, a highly abundant HLA type which was also included in our analysis [44].

To our knowledge, no CHIKV T-cell epitopes in humans have been described thus far. We predicted and, for the first time, experimentally identified multiple $CD4^+$ T-cell epitopes. Infection of human cell lines and vaccination of humanized transgenic mice with a recombinant vaccinia virus expressing CHIKV structural proteins (rVACV-CHIKV) led to the identification of multiple HLA class II-restricted epitopes [45,46]. One of the identified epitopes in the E2 structural protein (PPVIGREKFHSRP) partly overlaps with the epitope recognized by TCC 1-D9 of donor 1 (THPFHHDPPVIGREK) identified in our study. In MHC ligand assays PPVIGREKFHSRP was suggested to be presented by HLA-DRB1*04:04, HLA-DRB1*13:01, HLA-DRB3*01:01 and HLA-DRB4*01:01. We have shown experimentally and predicted that THPFHHDPPVIGREK can be presented by HLA-DRB1*04:01 and HLA-DRB1*03:01. Moreover, we found that THPFHHDPPVIGREK may also bind to HLA-DRB3*02:02 and HLA-DRB3*01:01. We predicted 8/9 experimentally identified $CD4^+$ T-cell epitopes and their HLA-restriction. However, regions previously *in silico* identified as immune-dominant based on the number of predicted epitopes per site, did not overlap with experimentally determined epitopes. Though *in silico* epitope predictions seem to be a good proxy for CHIKV-specific $CD4^+$ T-cell epitopes, the arbitrary chosen cut-off used to define immune-dominant regions seems less valuable in the prediction of CHIKV T-cell epitopes.

We were not able to isolate and expand CHIKV-specific $CD8^+$ TCC. A potential explanation could be a sub-optimal stimulation of $CD8^+$ T-cells by 15-mer peptides as usually shorter peptides are recognized by $CD8^+$ T-cells. Another possibility for the impaired induction of CHIKV-specific $CD8^+$ T-cells as observed in our study could be the participants' pre-existing anti-vector immunity. There is a large body of evidence that humoral responses induced by MV-CHIK are unimpeded by pre-existing immunity against the vector [15,19,20], but this aspect has not been addressed for cell-mediated immunity. While pre-existing immunity seems to not abolish CHIKV-specific $CD4^+$ T-cell induction, this could be the case for $CD8^+$ T-cells. A modified vaccinia virus Ankara (MVA)-based vaccine study in mice with pre-existing vector-specific immunity showed that pre-existing immunity prevented the induction of transgene-specific ($CD4^+$ and $CD8^+$) T-cell responses [47]. It remains to be investigated whether $CD8^+$ T-cells can be efficiently induced to different transgenes in the context of recombinant MV-vectored vaccines and if $CD8^+$ T-cell induction is dependent on pre-existing vector immunity.

Overall, we show that a MV-based CHIKV vaccine induced robust virus-specific $CD4^+$ T-cell responses in combination with consistent formation of CHIKV-specific antibodies as shown previously. Although we could not detect virus-specific $CD8^+$ T-cells after vaccination, the evidence for neutralizing antibodies as a correlate of protection indicates that a vaccine that induces a robust T helper response could be sufficient in the prevention of CHIKF.

Funding

K.S.S., R.D.d.V. and R.l.d.S. are supported by the Health~Holland grant EMCLSH19012 co-funded by the PPP Allowance made available by the Health~Holland, Top Sector Life Sciences & Health, to stimulate public–private partnerships. This project has been funded in part with Federal funds from the National Institutes of Health, under Contract No. 75N93019C00065 to D.W. and A.S.

CRediT authorship contribution statement

Katharina S. Schmitz: Conceptualization, Formal analysis, Investigation, Project administration, Resources, Visualization, Writing – original draft, Writing – review & editing. **Anouskha D. Comvalius:** Investigation, Writing – review & editing. **Nella J. Nieuwkoop:** Investigation, Writing – review & editing. **Daryl Geers:** Writing – review & editing. **Daniela Weiskopf:** Conceptualization, Investigation, Resources, Writing – review & editing. **Katrin Ramsauer:** Conceptualization, Funding acquisition, Investigation, Project administration, Resources, Supervision, Writing – review & editing. **Alessandro Sette:** Conceptualization, Investigation, Resources, Writing – review & editing. **Roland Tschismarov:** Funding acquisition, Investigation, Project administration, Resources, Supervision, Writing – review & editing. **Rory D. de Vries:** Conceptualization, Formal analysis, Funding acquisition, Investigation, Project administration, Supervision, Writing – review & editing. **Rik L. de Swart:** Conceptualization, Formal analysis, Funding acquisition, Investigation, Project administration, Supervision, Writing – review & editing.

Declaration of Competing Interest

The authors declare the following financial interests/personal relationships which may be considered as potential competing interests: R. L. de Swart reports financial support was provided by National Government of the Netherlands. A. Sette reports financial support was provided by National Institutes of Health. K Ramsauer, R Tschismarov reports a relationship with Merck & Co Inc that includes: employment.

Data availability

Data will be made available on request.

Acknowledgments

We thank the trial participants for their time and support.

Appendix A. Supplementary data

Supplementary data to this article can be found online at https://doi.org/10.1016/j.vaccine.2023.09.022.

References

[1] Halstead SB. Reappearance of chikungunya, formerly called dengue, in the Americas. Emerg Infect Dis 2015;21:557–61.
[2] Weaver SC. Prediction and prevention of urban arbovirus epidemics: a challenge for the global virology community. Antiviral Res 2018;156:80–4.
[3] Campion EW, Weaver SC, Lecuit M. Chikungunya virus and the global spread of a mosquito-borne disease. N Engl J Med 2015;372:1231–9.
[4] Rezza G, Weaver SC. Chikungunya as a paradigm for emerging viral diseases: evaluating disease impact and hurdles to vaccine development. PLoS Negl Trop Dis 2019;13:e0006919.
[5] Ndeffo-Mbah ML, Durham DP, Skrip LA, Nsoesie EO, Brownstein JS, Fish D, et al. Evaluating the effectiveness of localized control strategies to curtail chikungunya. Sci Rep 2016;6:23997.
[6] Yoon IK, Alera MT, Lago CB, Tac-An IA, Villa D, Fernandez S, et al. High rate of subclinical chikungunya virus infection and association of neutralizing antibody with protection in a prospective cohort in the Philippines. PLoS Negl Trop Dis 2015;9:e0003764.
[7] Yoon IK, Srikiatkhachorn A, Alera MT, Fernandez S, Cummings DAT, Salje H. Pre-existing chikungunya virus neutralizing antibodies correlate with risk of symptomatic infection and subclinical seroconversion in a Philippine cohort. Int J Infect Dis 2020;95:167–73.
[8] Srikiatkhachorn A, Alera MT, Lago CB, Tac-An IA, Villa D, Fernandez S, et al. Resolution of a chikungunya outbreak in a prospective cohort, Cebu, Philippines, 2012–2014. Emerg Infect Dis 2016;22:1852–4.
[9] Schmidt C, Schnierle BS. Chikungunya vaccine candidates: current landscape and future prospects. Drug Des Devel Ther 2022;16:3663–73.
[10] WHO. Measles fact sheet; 2019. https://www.who.int/news-room/fact-sheets/detail/measles?gclid=CjwKCAjwwL6aBhBlEiwADycBIEuGnWquH0gaTaPBRu4pT5Y9MjPpGrxk1uDEvsEhXg0t59FwhaRgsBoChLAQAvD_BwE.
[11] CDC. Measles vaccination; 2021. https://www.cdc.gov/vaccines/vpd/measles/index.html.
[12] Bautista-López N, Ward BJ, Mills E, McCormick D, Martel N, Ratnam S. Development and durability of measles antigen-specific lymphoproliferative response after MMR vaccination. Vaccine 2000;18:1393–401.
[13] Ebenig A, Lange MV, Mühlebach MD. Versatility of live-attenuated measles viruses as platform technology for recombinant vaccines. NPJ Vaccines 2022;7:119.
[14] Hu HM, Chen HW, Hsiao YJ, Wu SH, Chung HH, Hsieh CH, et al. The successful induction of T-cell and antibody responses by a recombinant measles virus-vectored tetravalent dengue vaccine provides partial protection against dengue-2 infection. Hum Vaccin Immunother 2016;12:1678–89.
[15] Brandler S, Ruffié C, Combredet C, Brault J-B, Najburg V, Prevost M-C, et al. A recombinant measles vaccine expressing chikungunya virus-like particles is strongly immunogenic and protects mice from lethal challenge with chikungunya virus. Vaccine 2013;31:3718–25.
[16] Mateo M, Reynard S, Pietrosemoli N, Perthame E, Journeaux A, Noy K, et al. Rapid protection induced by a single-shot Lassa vaccine in male cynomolgus monkeys. Nat Commun 2023;14:1352.
[17] Hörner C, Fiedler AH, Bodmer BS, Walz L, Scheuplein VA, Hutzler S, et al. A protective measles virus-derived vaccine inducing long-lasting immune responses against influenza A virus H7N9. NPJ Vaccines 2023;8:46.
[18] Rossi SL, Comer JE, Wang E, Azar SR, Lawrence WS, Plante JA, et al. Immunogenicity and efficacy of a measles virus-vectored chikungunya vaccine in nonhuman primates. J Infect Dis 2019.
[19] Ramsauer K, Schwameis M, Firbas C, Müllner M, Putnak RJ, Thomas SJ, et al. Immunogenicity, safety, and tolerability of a recombinant measles-virus-based chikungunya vaccine: a randomised, double-blind, placebo-controlled, active-comparator, first-in-man trial. Lancet Infect Dis 2015;15:519–27.
[20] Reisinger EC, Tschismarov R, Beubler E, Wiedermann U, Firbas C, Loebermann M, et al. Immunogenicity, safety, and tolerability of the measles-vectored chikungunya virus vaccine MV-CHIK: a double-blind, randomised, placebo-controlled and active-controlled phase 2 trial. Lancet 2018.
[21] Tschismarov R, Zellweger RM, Koh MJ, Leong YS, Low JG, Ooi EE, et al. Antibody effector analysis of prime versus prime-boost immunizations with a recombinant measles-vectored chikungunya virus vaccine. JCI Insight 2021;6.
[22] Grifoni A, Sidney J, Zhang Y, Scheuermann RH, Peters B, Sette A. A Sequence homology and bioinformatic approach can predict candidate targets for immune responses to SARS-CoV-2. Cell Host Microbe 2020;27. 671–80.e2.
[23] Carrasco Pro S, Sidney J, Paul S, Lindestam Arlehamn C, Weiskopf D, Peters B, et al. Automatic generation of validated specific epitope sets. J Immunol Res 2015;2015:763461.
[24] Weiskopf D, Schmitz KS, Raadsen MP, Grifoni A, Okba NMA, Endeman H, et al. Phenotype and kinetics of SARS-CoV-2-specific T cells in COVID-19 patients with acute respiratory distress syndrome. Sci Immunol 2020;5.
[25] Moosmann A, Khan N, Cobbold M, Zentz C, Delecluse H-J, Hollweck G, et al. B cells immortalized by a mini-Epstein-Barr virus encoding a foreign antigen efficiently reactivate specific cytotoxic T cells. Blood 2002;100:1755–64.
[26] Gonzalez-Galarza F, McCabe A, Santos ED, Jones J, Takeshita L, Ortega-Rivera N, et al. update: gold-standard data classification, open access genotype data and new query tools. Nucleic Acids Res 2020;48:D783-D8.
[27] Petitdemange C, Wauquier N, Vieillard V. Control of immunopathology during chikungunya virus infection. J Allergy Clin Immunol 2015;135:846–55.
[28] Poo YS, Rudd PA, Gardner J, Wilson JAC, Larcher T, Colle M-A, et al. Multiple immune factors are involved in controlling acute and chronic chikungunya virus infection. PLOS Neglected Trop Dis 2014;8:e3354.
[29] Wauquier N, Becquart P, Nkoghe D, Padilla C, Ndjoyi-Mbiguino A, Leroy EM. The acute phase of chikungunya virus infection in humans is associated with strong innate immunity and T CD8 cell activation. J Infect Dis 2010;204:115–23.
[30] Chua CL, Sam IC, Chiam CW, Chan YF. The neutralizing role of IgM during early chikungunya virus infection. PLoS One 2017;12:e0171989.
[31] Hoarau J-J, Jaffar Bandjee M-C, Krejbich Trotot P, Das T, Li-Pat-Yuen G, Dassa B, et al. Persistent chronic inflammation and infection by chikungunya arthritogenic alphavirus in spite of a robust host immune response. J Immunol 2010;184:5914–27.
[32] Kulkarni SP, Ganu M, Jayawant P, Thanapati S, Ganu A, Tripathy AS. Regulatory T cells and IL-10 as modulators of chikungunya disease outcome: a preliminary study. Eur J Clin Microbiol Infect Dis 2017;36:2475–81.
[33] Hoarau J-J, Gay F, Pellé O, Samri A, Jaffar-Bandjee M-C, Gasque P, et al. Identical strength of the T cell responses against E2, nsP1 and capsid CHIKV proteins in recovered and chronic patients after the epidemics of 2005–2006 in La Reunion Island. PLOS ONE 2013;8:e84695.
[34] Powers AM. Vaccine and therapeutic options to control chikungunya virus. Clin Microbiol Rev 2018;31:e00104-16.
[35] Khan M, Dhanwani R, Rao PVL, Parida M. Subunit vaccine formulations based on recombinant envelope proteins of chikungunya virus elicit balanced Th1/Th2 response and virus-neutralizing antibodies in mice. Virus Res 2012;167:236–46.
[36] Weger-Lucarelli J, Chu H, Aliota MT, Partidos CD, Osorio JE. A novel MVA vectored chikungunya virus vaccine elicits protective immunity in mice. PLOS Neglected Trop Dis 2014;8:e2970.
[37] Bao H, Ramanathan AA, Kawalakar O, Sundaram SG, Tingey C, Bian CB, et al. Nonstructural protein 2 (nsP2) of chikungunya virus (CHIKV) enhances protective immunity mediated by a CHIKV envelope protein expressing DNA vaccine. Viral Immunol 2013;26:75–83.
[38] Muthumani K, Lankaraman KM, Laddy DJ, Sundaram SG, Chung CW, Sako E, et al. Immunogenicity of novel consensus-based DNA vaccines against chikungunya virus. Vaccine 2008;26:5128–34.

[39] Chu H, Das SC, Fuchs JF, Suresh M, Weaver SC, Stinchcomb DT, et al. Deciphering the protective role of adaptive immunity to CHIKV/IRES a novel candidate vaccine against chikungunya in the A129 mouse model. Vaccine 2013;31:3353–60.
[40] Erasmus JH, Auguste AJ, Kaelber JT, Luo H, Rossi SL, Fenton K, et al. A chikungunya fever vaccine utilizing an insect-specific virus platform. Nat Med 2017;23:192–9.
[41] Roques P, Ljungberg K, Kümmerer BM, Gosse L, Dereuddre-Bosquet N, Tchitchek N, et al. Attenuated and vectored vaccines protect nonhuman primates against chikungunya virus. JCI Insight 2017;2:e83527.
[42] Mallilankaraman K, Shedlock DJ, Bao H, Kawalekar OU, Fagone P, Ramanathan AA, et al. A DNA vaccine against chikungunya virus is protective in mice and induces neutralizing antibodies in mice and nonhuman primates. PLoS Negl Trop Dis 2011;5:e928.
[43] Folegatti PM, Harrison K, Preciado-Llanes L, Lopez FR, Bittaye M, Kim YC, et al. A single dose of ChAdOx1 Chik vaccine induces neutralizing antibodies against four chikungunya virus lineages in a phase 1 clinical trial. Nat Commun 2021;12:4636.
[44] Lopes-Ribeiro Á, Araujo FP, Oliveira PdM, Teixeira LdA, Ferreira GM, Lourenço AA, et al. In silico and in vitro arboviral MHC class I-restricted-epitope signatures reveal immunodominance and poor overlapping patterns. Front Immunol 2022;13:1035515.
[45] Lorente E, Barriga A, Garcia-Arriaza J, Lemonnier FA, Esteban M, Lopez D. Complex antigen presentation pathway for an HLA-A*0201-restricted epitope from Chikungunya 6K protein. PLoS Negl Trop Dis 2017;11:e0006036.
[46] Lorente E, Barriga A, Barnea E, Palomo C, García-Arriaza J, Mir C, et al. Immunoproteomic analysis of a Chikungunya poxvirus-based vaccine reveals high HLA class II immunoprevalence. PLoS Negl Trop Dis 2019;13:e0007547.
[47] Altenburg AF, van Trierum SE, de Bruin E, de Meulder D, van de Sandt CE, van der Klis FRM, et al. Effects of pre-existing orthopoxvirus-specific immunity on the performance of modified vaccinia virus Ankara-based influenza vaccines. Sci Rep 2018;8:6474.